Twenty-Seventh Symposium (International) on Combustion/The Combustion Institute, 1998/pp. 2839–2846

PHYSICAL, THERMAL, AND CHEMICAL EFFECTS OF FINE-WATER DROPLETS IN EXTINGUISHING COUNTERFLOW DIFFUSION FLAMES

A. M. LENTATI AND H. K. CHELLIAH
Department of Mechanical, Aerospace and Nuclear Engineering
University of Virginia
Charlottesville, VA 22903, USA

A numerical method, based on a hybrid Eulerian–Lagrangian formulation for gas and droplet phase, is used here for the analysis of physical, thermal, and chemical effects of water droplets in extinguishing a methane-air non-premixed flame. The flow field considered here is a steady, laminar counterflow with monodisperse water droplets introduced with the air stream. The droplet sizes considered range from 5 to 50 μm, with maximum water-mass fraction in the condensed phase of 3%. The physical effects are analyzed by modifying the droplet trajectory and dilution. When the droplets are assumed to follow the gas exactly, the flame extinction results are shown to deviate considerably from the predictions obtained previously, where the flame extinction strain was shown to have a nonmonotonic dependence on droplet size. By decoupling the chemical effects associated with water, mainly the three-body recombination effects, it is shown here that the evaporated water vapor has less than 10% effect on the flame-extinction condition. In contrast, the thermal effects, mainly through the latent heat of vaporization, is shown to influence the flame-extinction condition significantly. Detailed comparisons of the flame structure obtained with water droplets and with that obtained using chemical agent halon 1301 are shown here to illustrate the completely different flame-suppression mechanisms of the two classes of agents.

Introduction

Effective fire-extinguishing agents are known to act primarily through chemical or thermal mechanisms (note: many authors consider thermal effects as part of general physical effects [1,2]). Because the chemical reaction rates are strong functions of temperature, quantifying the exact chemical and thermal contributions of these agents in extinguishing fires is not straightforward, especially by large-scale experiments and modeling. A laboratory-scale counterflow flame, with the provision for introducing gaseous or condensed-phase agents with the air stream, provides an excellent configuration for such experimental and theoretical studies [3–7] and is employed here. This paper analyzes and presents the numerical results of such a study, where the physical, thermal, and chemical effects of two class of agents (namely, fine-water droplets and halon 1301—CF_3Br) in extinguishing a non-premixed methane-air flame are quantified. The model developed as part of this work can be easily extended to other condensed-phase agents and to fuel-air systems as well.

Unlike gaseous agents, the effectiveness of condensed-phase agents depends on the dynamics of the droplets or particles in a given flow configuration. For the non-premixed counterflow configuration with fine-water droplets introduced with the air stream, the droplet dynamic effects were clearly shown in a recent numerical study [7]. The results of Ref. [7] indicated that when monodisperse droplets are introduced with the air stream, there is an optimal droplet size that maximizes the flame-extinction effectiveness, which is characterized by the extinction flow strain rate. For other droplet sizes, that is, lower or higher than this optimum size, with the mass of water in the condensed phase held fixed, flame extinction was observed to occur at higher strain rates, indicating the lower effectiveness. In the present investigation, these results are analyzed by systematically modifying the thermal and chemical parameters, as well as by modifying the dynamics of water droplets.

The theoretical model adopted here employs a hybrid Eulerian–Lagrangian formulation for gas-particle flow. For steady, planar axisymmetric flames established in the mixing layer of the counterflow field, and subjected to a standard set of approximations, the two-dimensional conservation equations for both gas and particles are reduced to a system of ordinary differential equations by introducing similarity approximations [7–12]. The version of simplified equations implemented here retains the more general rotational outer flow description to include the finite separation distance between the fuel and air stream. The flame considered is that established by two opposed streams of pure methane and air, with the fire-extinguishing agent introduced with the air stream. A detailed chemical kinetic mechanism and full

transport description are employed in the present model.

The present analysis clearly indicates that water droplets act primarily through thermal effects, with chemical effects contributing less than 10%. Qualitative arguments indicating the importance of such thermal effects of water have been presented before, but for the first time, this work presents a method of quantifying such contributions accurately. When water droplets and Halon 1301 are added, independently, so that the same flame-extinction strain rate is obtained, a comparison of the resulting flame structures for these two cases reveals interesting information about the role of rate-controlling chain-branching reaction. In addition, the important role of droplet dynamics is demonstrated by comparing a case where droplets are forced to follow the gas exactly with a realistic case where droplet trajectories are allowed to deviate from the gas.

Numerical Approach

Hybrid Eulerian–Lagrangian formulations for gas and particle phases have been employed previously in the context of fuel spray combustion in counterflow fields [12–14]. Such a technique has been extended recently to investigate the dynamics and flame-extinction effectiveness of fine-water droplets [7]. In this method, the gas-phase Eulerian equations are solved using a detailed chemical kinetic model and full thermodynamic and transport description, and coupled with droplet source terms. Knowing the gas-phase solution, the Lagrangian equations for mass, momentum, energy, and particle flux fraction (defined as the droplet flux normalized by that at the air nozzle exit) are integrated in time to determine the droplet location and source terms contributing to the gas-phase equations. For simplicity of analysis, only monodisperse droplets are considered in the present work, with different initial droplet sizes. The sizes considered range from 5 to 50 μm diameters. For brevity, only the droplet equations are reported here to indicate the source terms contributing to the gas-phase equations that are modified as part of this analysis. For a single droplet, with low droplet Reynolds number (based on the velocity lag between the droplet and the gas), the Lagrangian equations controlling the mass, momentum in axial and radial directions, and enthalpy can be written as [7]

$$\frac{dm_d}{dt} = -Q \tag{1}$$

$$\frac{d}{dt}(m_d v_d) = -Q v_d + 3\pi d\bar{\mu}(v - v_d) \tag{2}$$

$$\frac{d}{dt}(m_d U_d) + m_d U_d^2 = -Q U_d + 3\pi d\bar{\mu}(U - U_d) \tag{3}$$

$$\frac{d}{dt}(m_d h_d) = -Q(h_d + L) + H \tag{4}$$

where m_d is the mass of the droplet, Q the mass evaporation rate, v_d the velocity of the droplet in axial direction identified here as x, U_d is a function of x only and is defined as u_d/r_d (with u_d the radial velocity of the droplet and r_d the initial radial location exiting the air stream), $\bar{\mu}$ the gas viscosity averaged over the viscous boundary layer of the droplet, h_d the enthalpy of the droplet, L the latent heat of vaporization of water, and H the heat flux to the droplet from the gas. The source terms on the right-hand side of equations 1–4 are coupled to the gas phase through the local droplet number density in a systematic manner [7], and the resulting gas-phase Eulerian equations are then integrated using Smooke's counterflow code [15,16]. For the outer frozen flow, the more general rotational flow description is employed [8–11]. In the present implementation, the two sets of coupled equations are iterated until a predetermined convergence criterion is reached [7]. The main advantage of using the Lagrangian formulation is to avoid the occurrence of singularity associated with the particle number density equation at the point where droplet trajectory is reversed [7,17].

For the methane fuel considered here, an elementary reaction mechanism involving 16 species in 39 steps is employed to describe its oxidation process [18]. The CF_3Br submechanism is the same as that employed in a previous study [6], containing an additional 17 species in 42 elementary reactions, which was adopted from Ref. [19]. The water evaporated from the droplets can modify the three-body collision efficiencies and the balance of reactions in equilibrium, in particular the water–gas shift reaction. In order to analyze the chemical effects associated with these modifications, the water evaporated from droplets is labeled as a different compound (identified here as H_2^*O) having the same thermal and physical properties as water but with no participation in chemical reactions.

Results and Discussion

The main advantage of pursuing theoretical studies as described here is of the ability to probe different physical, thermal, and chemical effects described in the Introduction by performing parametric studies. However, complete decoupling of various contributing effects is not possible because of the nonlinearity of the problem being investigated and should be emphasized here.

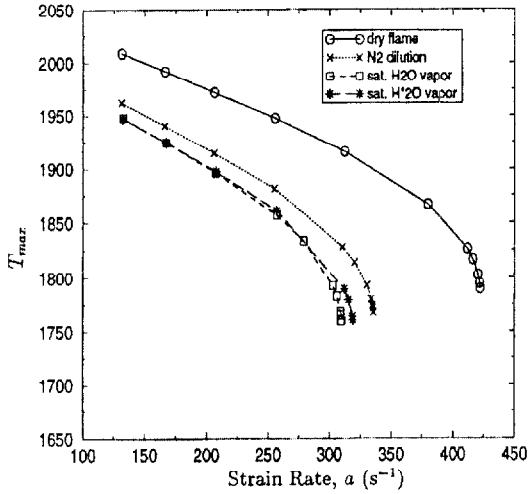

FIG. 1. Comparison of T_{max} versus a, for dry cases (○), diluted cases with saturated water vapor (□), water vapor excluded from chemistry (*), and nitrogen (×).

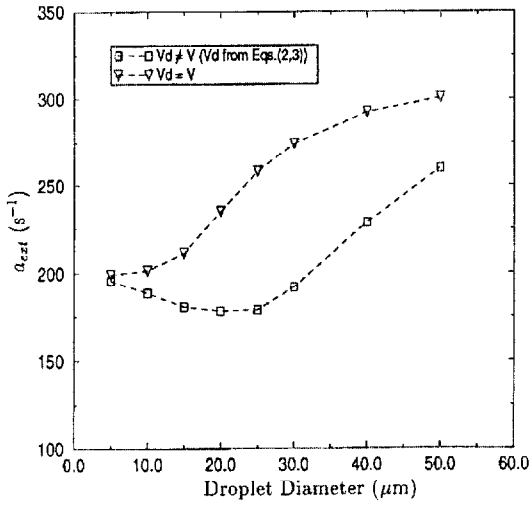

FIG. 2. Variation of extinction strain rate as a function of droplet size, when droplets follow the gas exactly (▼) and when trajectories are determined from equations 2 and 3 (□).

Physical Effects

Whether it is a small-scale or large-scale fire, when water droplets are introduced with the air stream, the air stream becomes saturated with water vapor. At room temperature of 300 K and atmospheric pressure, the saturated water vapor in air is 3.51% by moles or 2.24% by mass. The dilution or displacement of the oxygen content in the air stream by this water vapor can have a considerable effect of the flame-extinction condition (about 25% reduction in the extinction strain rate) and is shown in Fig. 1, where the variation of maximum flame temperature is plotted as a function of flow strain rate. For the rotational outer flow field employed in the present calculations, the strain rate, a, is defined as the negative axial velocity gradient in the axial direction (i.e., $a = -dv/dx$) in the oxidizer side, closer to the mixing layer [11]. In Fig. 1, the symbol (○) indicates the dry flame solution, and the symbol (□) identifies that obtained by replacing the oxygen and nitrogen content in the air stream proportionately with water vapor. For comparison, a case where the water vapor is replaced by nitrogen with the same mole fraction is also shown in Fig. 1 by symbol (×). The difference between the water vapor (symbol □) and nitrogen (symbol ×) dilution can be attributed to the specific heat effects, but the difference between the dry case (symbol ○) and water vapor (symbol □) case is due to combination of diffusional and shift in flame location effects, a reason for considering these as physical effects. Also shown in Fig. 1 is a case where the saturated water vapor introduced with the air stream is excluded in chemical reactions by identifying it as different compound H_2^*O, indicating the minor chemical role.

Another source of physical effect arising from water droplets is the source terms contributing to the gas-phase momentum equation, which are found to be negligible for small-droplet loading considered here (maximum of 3% by mass in condensed phase). The departure of the droplet trajectory from the gas can also be considered as a physical phenomenon, but effects arising from it are somewhat difficult to decouple from the thermal or chemical effects described later. To demonstrate the importance of particle trajectory, a case where the droplets are assumed to follow the gas exactly irrespective of their size is considered, and the predicted flame-extinction results as a function of droplet sizes are shown in Fig. 2, for 2% by mass of water in condensed phase (symbol ▽). These results indicate a *monotonic* variation of extinction strain rate as a function of droplet size, which is quite different from that obtained when the droplets are allowed to deviate from the gas flow (symbol □). The reason for the observed differences between the two cases shown in Fig. 2 is related to the droplet dispersion in the counterflow field. For example, when the droplets follow the gas exactly, the droplets spread rapidly as the stagnation plane is approached as compared to the case where droplet trajectory is determined by integrating the Lagrangian equations subjected to viscous drag terms given by equations 2 and 3. Similar results are obtained for other droplet mass loadings, indicating the need to accurately model the droplet trajectories. Because the droplet trajectories obtained by the integration of equations 2 and 3 represent the actual situation, only this case is considered in the remaining sections of this paper.

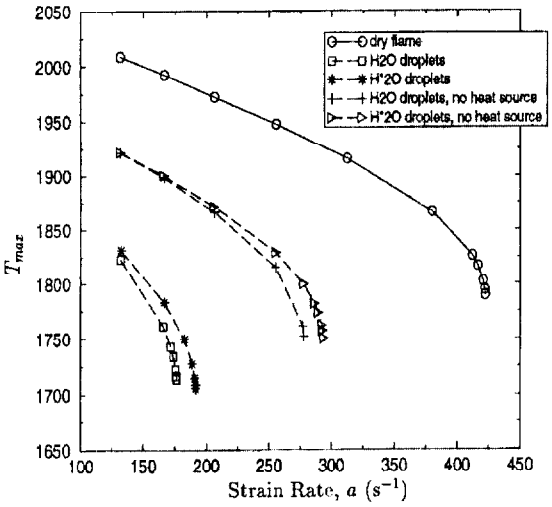

FIG. 3. Comparison of T_{max} versus a, for dry cases (○) and 2% by mass of 20-μm water droplets, with chemical effects modified (*, ▷) and thermal effects modified (+, ▷).

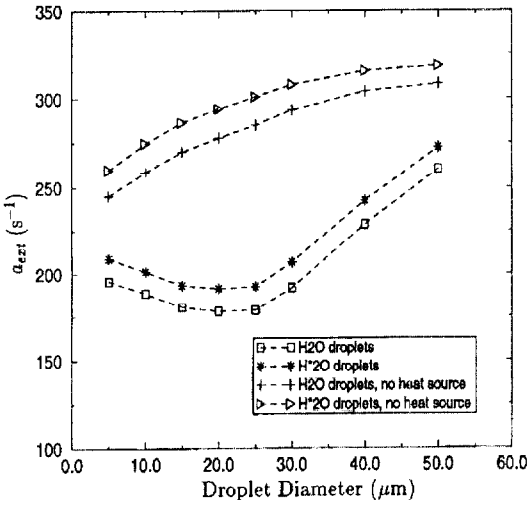

FIG. 4. Variation of extinction strain rate as a function of droplet size, with chemical and thermal effects modified.

Chemical and Thermal Effects

The evaporated water can participate in homogeneous chemical reactions and affect the flame-extinction phenomena. Gaseous water is known to have a much higher three-body collisional efficiency (a factor of 16 higher compared to nitrogen [20]), and hence can enhance the radical recombination process leading to lower extinction strain rates. High water concentrations in the gas phase can also affect the water–gas shift reaction. In order to analyze the chemical effects associated with droplet evaporation given by Q in equation 1, as compared to that produced by methane oxidation (typically about 18% by mass [16]), the former is identified here as H_2^*O, and its participation in gas-phase chemical reactions can be selectively turned on or off. For 2% by mass of 20-μm water droplets, the resulting variation of the maximum flame temperature as a function of flow strain rate is shown in Fig. 3, where the symbol (□) includes the effect of water in all chemical reactions and the symbol (*) excludes such effects. The small difference seen between these two lines indicate that the three-body recombination effects have a minor effect on the flame-extinction condition, consistent with Fig. 1 where only saturated water vapor was added to the air stream. The water evaporated from droplets is seen to weaken the overall combustion process and thereby reduce the extinction condition slightly, rather than enhance the combustion process.

Unlike the chemical effects of water droplets, the role of thermal effects of water droplets, associated with latent heat of vaporization and increase in the sensible enthalpy of condensed water droplets from room temperature to local droplet temperature [i.e., the term $-Q(h_d + L) + H$ in equation 4], together with the modification of gas-phase enthalpy due to addition of water vapor (i.e., $Qh_{H_2O,g}$), can be easily analyzed in the present simulations by setting the net source term contributing to the gas-phase equations, $Q(h_d + L) - H - Qh_{H_2O,g}$, equal to zero. This modification on the maximum flame-temperature predictions is shown in Fig. 3 by symbols (+) with water evaporated participating in gas-phase reactions and symbol (▷) with water evaporated not participating in gas-phase reactions. The foregoing analyses clearly indicate that the neglect of the source term $Q(h_d + L) - H - Qh_{H_2O,g}$ in gas-phase equations increases the flame-extinction condition from 176 to 255 s^{-1}, whereas the neglect of water in chemical reactions changes the extinction strain rate from 176 to 190 s^{-1}.

Figure 4 shows a comparison of the previous extinction strain-rate results for selected monodisperse droplet sizes, with 2% by mass water in the condensed phase. Here, symbol (□) indicates when thermal and chemical effects are included and symbol (▷) indicates when both thermal and chemical are excluded. The latter case corresponds to a dilution effect. Also shown in the same figure are those obtained when chemical effects of water originating from the air stream are only turned off (symbol *) and thermal effects of water droplets are only turned off (symbol +). Most interesting feature is that the removal of thermal effects leads to a monotonic variation of extinction strain (symbols + and ▷). This monotonic decrease in extinction strain rate with droplet size is due to the increasing amount of dilution of air, which depends on how rapidly the water droplets evaporate before approaching the flame

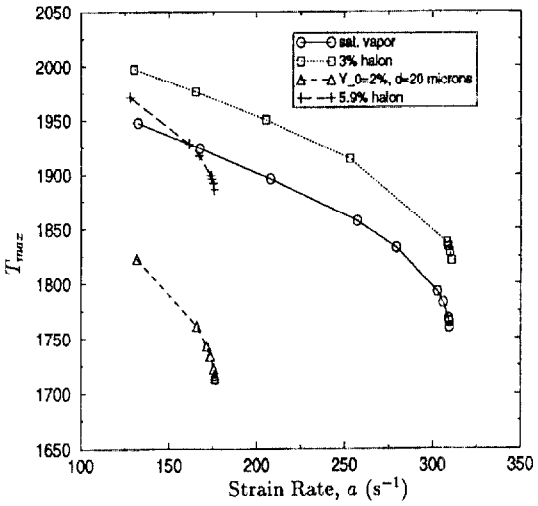

FIG. 5. Comparison of T_{max} versus a, for halon 1301 of 3% (□) and of 5.9% (+), saturated water vapor of 2.24% (○), and condensed-phase water of 2% + saturated vapor of 2.24% (△).

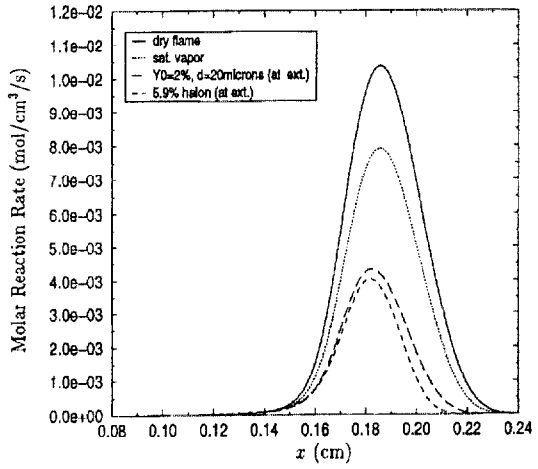

FIG. 6. The variation of reaction $H + O_2 \rightarrow OH + O$ versus axial distance at an extinction strain rate of 176 s^{-1}, for halon 1301 (short dash) and water droplets (long dash). Also shown is the dry case (solid line) and saturated water vapor case (dotted line) at the same strain rate.

front. For example, 5-μm droplets are found to vaporize rapidly as soon as they enter the mixing layer [7] and thereby dilute the oxidizer boundary conditions. In the case of 50-μm droplets, for the same mass of water in the condensed phase leaving the air nozzle, only a small fraction of the water is evaporated before reaching the flame, and the remainder is convected away from the flame, which explains their reduced effectiveness as seen by higher extinction strain rate.

The removal of chemical effects has a small effect on extinction strain rate as indicated by the difference between symbols (□) and (*) or (+) and (▷). The inclusion of thermal effects is seen to decrease the extinction strain rates significantly, leading to a nonmonotonic dependence on the droplet size, as indicated by symbols (□) and (*). Aside from these thermal effects, the nonmonotonic behavior observed is found to be strongly coupled to the dynamics of the droplets (see Fig. 2), which determines the critical particle size that is most effective in suppressing the counterflow flames considered here.

Comparisons with Halon 1301

In addition to the aforementioned global effects on flame-extinction condition, the influence of water droplets on finite-rate chemical reactions is analyzed here and compared with those obtained with the gaseous chemical agent halon 1301 or CF_3Br.

Previous numerical studies using detailed chemical kinetic models [16] and theoretical studies using reduced reaction models [11,21] have clearly indicated that the extinction flow strain rate of methane-air non-premixed flames are controlled by the finite rate of radical species production, which can also be related to the oxygen consumption through the reaction $H + O_2 \rightarrow OH + O$. Both water droplets and halon 1301 are expected to modify this reaction and thereby reduce the flame extinction strain rate. Because of the thermal and chemical effects of these two agents, the influence on the flame structure can be quite different and is analyzed here.

Figure 5 shows a comparison of the variation of maximum flame temperature as a function of strain rate predicted with 2% by mass of 20-μm water droplets and with 5.9% by mass halon 1301 (symbol +). Here 2% of water in the condensed phase is in addition to the saturated water vapor of 2.24% by mass in the air stream. For comparison, the saturated water vapor case shown in Fig. 1 by symbol (□) and a case with 3% by mass halon 1301 (symbol ○) is also shown. The mass fractions of water droplets and halon 1301 were considered such that they yield the same extinction strain rate of about 176 s^{-1}. At flame extinction, as seen in Fig. 5, the maximum flame temperature of the halon 1301 case is almost 200 K higher than the predictions with water droplets. The rates of the key chain-branching reaction $H + O_2 \rightarrow OH + O$, however, indicate a very similar value across the flame front for both agents, as shown in Fig. 6. Again for comparison, at the same flow strain rate, variations of the reaction $H + O_2 \rightarrow OH + O$ for the dry case and the saturated water vapor case are also shown. Because this reaction is the key chain-branching reaction producing radical species, these results are consistent with the earlier statement that flame extinction of methane-air non-premixed flames are controlled by the finite rate of

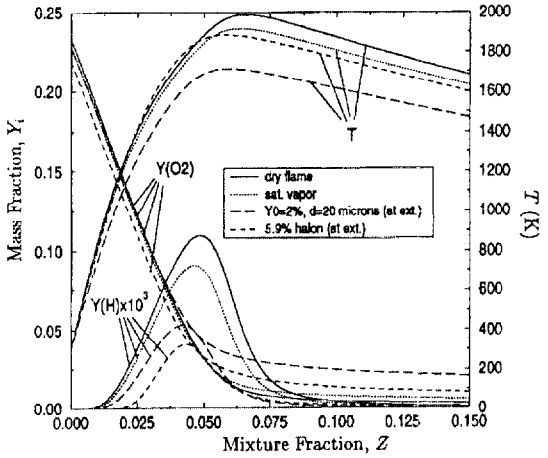

FIG. 7. The variation of H-atom and oxygen mass fractions, and temperature versus mixture fraction at an extinction strain rate of 176 s^{-1}, for halon 1301 (short dash) and water droplets (long dash). Also shown is the dry case (solid line) and saturated water vapor case (dotted line) at the same strain rate.

radical production or oxygen-consumption reaction, irrespective of addition of either thermal or chemical fire-extinguishing agents.

Although the peak flame temperature between water droplets and halon 1301 differ by about 200 K at extinction, the fact that the reaction rate of $H + O_2 \rightarrow OH + O$ remains the same can be explained from the following considerations. As the flow strain rate is increased, the reduction of flow residence time leads to a decrease in oxygen consumption. Consequently, part of the oxygen leaks through the flame, as shown in Fig. 7. Furthermore, the mass fraction of oxygen at the peak radical production region at flame extinction is typically found to be the same. Thus, the only mechanism by which the reaction rate of $H + O_2 \rightarrow OH + O$ remains the same at extinction is by having two different levels of H-atom concentration, for the two distinct classes of agents considered. This can be clearly illustrated by plotting the flame temperature and H-atom mass-fraction variations across the non-premixed flame, as shown in Fig. 7. These results clearly indicate that halon 1301 acts to reduce the radical pool—characteristic of chemical fire-suppressing agents, and as a result, for a given flow strain rate or flow residence time, the flame extinction occurs at a relatively high flame temperature. In contrast, water droplets reduce the flame temperature through thermal effects, and flame extinction occurs at a higher level of H-atom mass fraction, as seen in Fig. 7.

Interestingly, on a mass basis, the 20-μm water droplets are slightly more effective than halon 1301 in extinguishing the counterflow diffusion flame considered here (i.e., 4.24% by mass total water added versus 5.9% by mass halon 1301). These results need to be validated with future experiments. Unlike halon 1301, which is a gaseous chemical agent, the optimum fine-water droplet size predicted is highly system or flow-field dependent. Thus, in scaling up from the present counterflow field to large-scale fires, the effect of droplet dynamics in the real flow field and the corresponding optimum droplet size must be carefully considered.

Conclusions

The purpose of this work was to analyze recent results obtained with a two-phase numerical model developed to understand the dynamics of water droplets in a counterflow field. In particular, the interesting nonmonotonic flame-extinction strain-rate prediction as a function of droplet size was analyzed by introducing systematic modifications of rate-controlling parameters.

The assumption of droplets following the gas exactly, irrespective of their size, was shown to reduce the flame-extinction effectiveness as the droplets are convected rapidly away from the flame. This assumption was also shown to affect the nonmonotonic variation of flame-extinction strain rate observed when droplet trajectories are solved independently using the Lagrangian equations of motion with viscous drag forces. By decoupling the chemical effects associated with water and turning off the thermal cooling effects associated with water evaporation and droplet heating, it was shown that for 20-μm droplets with 2% by mass in the condensed phase, the thermal cooling effects alone reduce the extinction strain rate by 40%, whereas chemical effects reduce the extinction strain rate by less than 10%.

Comparisons of the flame-extinction condition and flame structure between water droplets and halon 1301 were also made to illustrate the two distinct extinction mechanisms by the two classes of agents. Water droplets were shown to reduce the radical production or oxygen consumption through decrease in flame temperature, whereas halon 1301 was shown to reduce the radical concentration through well-known chemical mechanisms. For the counterflow non-premixed flames considered here, it was shown that on a mass basis, water droplets are slightly more effective in extinguishing the flame when compared with halon 1301. Experimental studies are currently underway to establish these predictions, and once the present model is validated, it will provide a valuable tool to develop new and more effective fire suppressants.

Acknowledgments

This work is supported by National Institute of Standards and Technology, Gaithersburg, MD, with Drs. William Grosshandler and Gregory Linteris as technical monitors.

REFERENCES

1. Friedman, R. and Levy, J. B., "Survey of Fundamental Knowledge of Mechanisms of Action of Flame Extinguishing Agents," WADC technical report 56-568, Wright Air Development Center, Wright-Patterson AFM, OH, January 1957.
2. Pitts, W. M., Nyden, M. R., Gann, R. G., Mallard, W. G., and Tsang, W., "Construction of an Exploratory List of Chemicals to Initiate the Search for Halon Alternatives," NIST tech. note 1279, August 1990.
3. Seshadri, K. and Williams, F. A., "Effect of CF_3Br on Counterflow Combustion of Liquid Fuel with Diluted Oxygen," in *ACS Symposium Series, No. 16, Halogenated Fire Suppressants* (R. G. Gann, ed.), American Chemical Society, Washington, D.C., 1975, p. 149.
4. Seshadri, K., *Combust. Flame* 33:197 (1978).
5. Hamins, A., Gmurczyk, G., Grosshandler, W., Presser, C., and Seshadri, K., "Flame Suppression Effectiveness," in *Evaluation of Alternate In-Flight Fire Suppressants for Full-Scale Testing in Aircraft Engine Nacelles and Dry Bays* (W. L. Grosshandler, R. G. Gann, and W. M. Pitts, eds.), NIST SP-861, April 1994.
6. Hamins, A., Trees, D., Seshadri, K., and Chelliah, H. K., *Combust. Flame* 99:221 (1994).
7. Lentati, A. M. and Chelliah, H. K., "Dynamics of Water Droplets in a Counterflow Field and Their Effect on Flame Extinction," *Combust. Flame* 115:158 (1998).
8. Seshadri, K. and Williams, F. A., *Int. J. Heat Mass Transfer* 21:251 (1978).
9. Kee, R. J., Miller, J. A., Evans, G. H., and Dixon-Lewis, G., in *Twenty-Second Symposium (International) on Combustion*, The Combustion Institute, Pittsburgh, 1988, p. 1479.
10. Smooke, M. D., Crump, J., Seshadri, K., and Giovangigli, V., "Comparison between Experimental Measurements and Numerical Calculations of the Structure of Counterflow, Diluted, Methane-Air, Premixed Flames," Yale University report ME-100-90, 1990.
11. Chelliah, H. K., Law, C. K., Ueda, T., Smooke, M. D., and Williams, F. A., in *Twenty-Third Symposium (International) on Combustion*, The Combustion Institute Pittsburgh, 1990, p. 503.
12. Continillo, G. and Sirignano, W. A., *Combust. Flame* 81:325 (1990).
13. Lacas, F., Darabiha, N., Versaevel, P., Rolon, J. C., and Candel, S., in *Twenty-Fourth Symposium (International) on Combustion*, The Combustion Institute, Pittsburgh, 1992, p. 1523.
14. Chen, N.-H., Rogg, B., and Bray, K. N. C., in *Twenty-Fourth Symposium (International) on Combustion*, The Combustion Institute, Pittsburgh, 1992, p. 1513.
15. Smooke, M. D., *J. Comp. Phys.* 48:72 (1982).
16. Smooke, M. D., Puri, I. K., and Seshadri, K., in *Twenty-First Symposium (International) on Combustion*, The Combustion Institute, Pittsburgh, 1986, p. 1783.
17. Li, S. C., Libby, P. A., and Williams, F. A., *Combust. Flame* 94:161–177 (1993).
18. Peters, N. and Rogg, B., *Reduced Kinetic Mechanisms for Applications in Combustion Systems*, Lecture Notes in Physics, Vol. m15, Springer-Verlag, New York, 1993.
19. Westbrook, C. K., *Combust. Sci. Technol.* 34:201–225 (1983).
20. Warnatz, J., in *Combustion Chemistry* (W. C. Gardiner Jr., ed.), Springer-Verlag, New York, 1984.
21. Seshadri, K. and Peters, N., *Combust. Flame* 73:23 (1988).
22. Chelliah, H. K. and Williams, F. A., *Combust. Flame* 60:17 1990.

COMMENTS

Daniel Dietrich, NASA Lewis Research Center, USA. Your simulation is for a mono-sized droplet spray. Comment on the effect the droplet-size distribution in a ploydisperse spray (more practical) would have on the extinction conditions. Specifically, would there be a mean size that characterized the spray (i.e., D_{10}, D_{20}, D_{32}, D_{30}), and if so, would there be an optimal size as with the mono-sized spray?

Author's Reply. In polydisperse sprays, in addition to the mean droplet size, the size distribution itself will play an important role in characterizing the optimal droplet size that controls flame extinction. Hence, monodisperse sprays are useful in understanding the individual size effects, as considered in our initial study. Because most practical sprays are polydisperse, we plan to extend our model to such polydisperse systems in the future. It is safe to speculate that the polydispersivity will smooth out the non-monotic variation of flame extinction *vs.* mean particle size, unlike the results presented in this paper.

•

Richard K. Lyon, Energy and Environmental Research Corporation, USA. Your conclusion, that fine water mist is more effective than CF_3Br for extinguishing fires, is, I believe, correct but misleading. After the mice decided that putting a bell around the cat's neck would protect them, they, so the story goes, faced the problem of getting the bell where it was needed. Similarly, getting fine mist to fires is a problem.

Author's Reply. Fine-water mist systems with much lower droplet settling velocities (in comparison with traditional water sprinkler systems) are supposed to work as a total flooding agent, similar to halon 1301. Although the mist will not diffuse to the flame front, these fine droplets are known to transport convectively with the airstream into the flame front and cause flame extinction. How effectively this will work for different flow configurations is beyond the scope of the present study and need further investigation.

•

James Quintiere, University of Maryland, USA. Can you explain how the domain or range of your strain rate might apply to applications such as natural fires, jet engine fires, and the standardized tests such as the cup burner test and the extinction complications of your results?

Author's Reply. In more realistic fire applications, as those cited by Dr. Quintiere, there will be a critical region that facilitates flame holding or anchoring. In these real fires, at flame extinction, a local flow strain rate can be identified in flame-holding regions that corresponds to the extinction strain rate of the counterflow flames investigated here. For the same extinction flow strain rate of the two systems (i.e., real fires and counterflow flames), the mass loading of the agent required for extinction of the two systems should be the same. Thus, the present results can be directly extrapolated to such real systems. However, in many real systems, the flow is not laminar as assumed here, for example, the presence of turbulent transport and turbulent–chemistry interactions can alter similarities between the two systems and should be taken into account when comparisons are made.

•

Kuldeep Prasad, Naval Research Laboratory, USA.

1. Your results indicate an optimum droplet diameter of 20 μm. What are the effects of inlet velocity (air and fire), droplet inlet velocity, and temperature on the optimum droplet diameter?
2. Have you performed any calculations with polydisperse droplets and droplet diameters greater than 100 or 150 μm?

Author's Reply. As mentioned in our paper, the optimum droplet diameter of 20 μm is obtained when we assumed that the velocity lag between the gas and the droplet is zero. Certainly, we can perform many parametric studies on the effect of velocity lag, droplet temperature, etc., but we have refrained from such investigations until experimental data are available to validate our model.

With regard to the second question, because of the small separation distance (typically 10–12 mm) between the air and fuel streams of counterflow systems, we find that droplets larger than about 100 μm penetrate the stagnation plane and have sufficient momentum to enter the fuel stream. Because of possible fuel stream contamination, we have restricted our investigations to the sizes indicated in the paper.

•

Ronald S. Sheinson, Naval Research Laboratory, USA. Our empirical physical action model [1] shows that ideal water-mist extinguishment of a heptane fire requires approximately 2/3 the mass of Halon 1301 required for extinguishment. However, our model, as does this Symposium paper, assumes the water–air mixture extinguishes the flame in one air volume-filling cycle. The authors do qualify the burner for which their conclusion applies.

For halon replacement, the reality is that the non-gas-like droplets rely on fire-generated convection for entrainment into small, obstructed diffusion flame fires. These fires are typically controlled but not extinguished. Major fire reignition from these pilot fires remains a hazard. Continuous water-mist generation must be maintained (droplet fallout) until trained and equipped response team intervention. Consequently, water-mist systems guaranteeing fire extinguishment typically require a greater agent mass than do hydrofluorocarbon gaseous agent systems and definitely more than do halon 1301 systems.

REFERENCE

1. Sheinson, R. S., Penner-Hahn, J. E., and Indritz, D., *Fire Safety J.* 15:437–450 (1989).

Author's Reply. As pointed out by Dr. Sheinson, in our paper, we explicitly indicate the importance of flow-field effects, particularly the limitation of present results to counterflow field. In the case of real fires, we completely agree that the droplet entrainment or transport phenomena must be carefully addressed, but the main focus of the present paper was to develop and validate a model that could quantify the various contributions arising from droplet interactions with laboratory-type flames.